

TEST PLAN

**HIGH-BURNUP SNF CLADDING INTEGRITY DURING CASK
TRANSPORTATION ACCIDENTS FOLLOWING DRYING, TRANSFER,
AND LONG-TERM STORAGE**

**Irradiation Performance Section
Nuclear Engineering Division
Argonne National Laboratory
Argonne, IL 60439**

November 26, 2007

**Test Plan for
High-Burnup SNF Cladding Integrity during Cask Transport Accidents following Drying,
Transfer and Long-Term Storage
November 26, 2007**

Executive Summary

This test plan is designed to meet the high-burnup-cladding data needs of (1) applicants for transportation package licenses (Industry); (2) DOE-RW, who will be purchasing a large number of transport casks; and (3) NRC-NMSS license-application technical reviewers. As such, all three organizations have participated in providing financial resources (NRC and DOE-RW) and high-burnup cladding (NRC and EPRI), as well as guidance on data needs. NRC has continued to provide financial support, while DOE-RW funding was discontinued in October 2005. Current NRC guidelines (SFPO ISG-11, Rev. 3) for high-burnup (>45 GWd/MTU) fuel limit the peak cladding temperature to $\leq 400^{\circ}\text{C}$ during normal handling, drying, transfer and storage of spent fuel. However, generic acceptance criteria do not exist for transportation of high-burnup commercial SNF. Licensing of such casks and packages are being handled on a case by case basis until further regulatory guidance is developed. In the context of this project, NRC-NMSS has specifically requested data on the axial tensile properties and impact resistance of high-burnup Zircaloy, ZIRLO and M5 cladding alloys to form the basis for assessing the performance of these cladding alloys during post-storage transportation accidents. The thermal and hoop-stress history of high-burnup cladding during drying/transfer and long-term storage may have a significant effect on cladding performance during post-storage transport accidents, particularly the hypothetical accident conditions (HAC) described in 10 CFR 71.73.

Maintaining cladding integrity is generally required under normal and off-normal conditions of storage and transportation, but not necessarily under accident conditions (unless criticality calculations assume intact fuel rods). However, assurance that cladding integrity would be maintained under most credible events would greatly simplify the preparation of a license application and its review. Overall, the data generated in this project are intended to be used, along with appropriate modeling codes, for assessing whether or not cladding is likely to fail in transport, to assess the failure mode, and to assess the axial extent of failure along fuel rods.

High-burnup cladding is degraded by radiation-induced hardening and hydrogen pickup, which occur during reactor operation. Radiation hardening, which is expected to saturate after a couple of reactor cycles, causes an increase in tensile strength and a decrease in ductility (i.e., plastic failure strain). Hydrogen pickup, which continues to increase with burnup, causes a further decrease in tensile ductility. In general, high-burnup cladding is anticipated to have some plastic ductility, which tends to inhibit fragmentation-mode failure during bending and crush-impact loading caused by cask-drop accidents. This has been demonstrated by previous test results generated in the ANL program using high-burnup Zry-4 cladding with a water-side corrosion layer $\leq 100\text{-}\mu\text{m}$ thick, hydrogen content <800 wppm, a dense rim of circumferential hydrides under the corrosion layer, and decreasing density of circumferential hydrides from cladding outer-to-inner surface. The expectation for such cladding in which hydrogen precipitates in the circumferential direction during cooling from drying temperatures ($\leq 400^{\circ}\text{C}$) to post-storage temperatures ($\approx 150\text{-}250^{\circ}\text{C}$) is that ductility and impact-resistance will be maintained

if hydrogen precipitates in the circumferential direction. However, drying operations, particularly those involving temperature cycling under high internal pressure, can result in reorientation of hydrogen precipitation from the circumferential to the radial direction. Cladding with high radial-hydride fraction and/or high radial-hydride "continuity" factor (measure of effective length of radial hydrides) is susceptible to brittle failure under impact hoop-stress loading expected during a side-drop accident.

The Test Plan includes high-burnup-cladding axial tensile tests conducted at 0.1 and 100%/s strain rate and RT-400°C. The reference conditions for these tests are 100%/s strain rate (25-mm/s displacement rate) and 150°C. These tests are performed at ANL using defueled cladding samples. In addition, ring-compression tests and crush impact tests are performed at ANL with prehydrided and defueled high-burnup cladding samples to assess failure ductility and energy following simulated drying conditions. A large number of tests are specified in this plan using prehydrided cladding in order to determine cooling conditions that are likely to induce radial hydride precipitation. Pressurized-and-sealed rodlets are used for this radial hydride treatment (RHT). The rodlets are cooled from 400°C at a slow rate (5°C/h) to determine the extent of radial hydride formation vs. hoop stress (≤ 150 MPa) at 400°C. This hoop stress decreases with temperature during cooling to simulate the thermal-stress history of a SNF rod. Prior to pressurization, the prehydrided cladding is annealed for 72 h at 400°C. The reference hold time at 400°C for the pressurized rodlet is 1 hour. Some of the rodlets are subjected to 9 thermal of $>65^\circ\text{C}$ with a 6-minute hold time at 400°C between cycles to determine the effects of such cycling on radial hydride formation. ISG 11, Rev. 3, limits thermal cycling to <10 cycles for $>65^\circ\text{C}$ temperature drop per cycle. Rings (8-mm-long) are sectioned from the rodlet and subjected to displacement-controlled ring-compression tests and ring crush-impact tests. The reference conditions for the ring-compression tests with prehydrided cladding are: 10-mm/s displacement rate (equivalent to $\approx 100\%$ /s diametral stain rate in loading direction); 2-mm maximum displacement; and both RT and 150°C. The crush impact tests are conducted at RT and a velocity of 2 m/s with a 2-mm maximum cladding displacement in the radial direction. For rings that develop radial cracks $\geq 20\%$ of the wall thickness at ≤ 2 -mm diametral displacement, absorbed energies from the two test types are compared to determine if the RHT-cladding cracking and/or failure energies are strain-rate sensitive. If they are not, then only ring-compression tests will be conducted at 150°C using high-burnup cladding samples following RHT.

Pressurized-and-sealed rodlets will also be used for RHT of defueled high-burnup cladding. The hoop-stress range and thermal history for these will be determined based on results for prehydrided cladding. High-burnup cladding rings will be compressed at 150°C and 10-mm/s displacement rate to 2-mm maximum displacement. For RHT conditions that result in $\geq 20\%$ and $<100\%$ through-wall cracking, the cracked rings will be subjected to ring-expansion tests to determine the internal pressure that would cause through-wall failure. Sibling samples will also be tested at 250°C to determine if there is a ductile-to-brittle transition in this temperature range.

The ANL test results will be used to plan the integral fueled-cladding tests to be conducted at ORNL. Currently planned tests consist of RT bend and impact tests using fueled-cladding segments that are ≈ 150 -mm long. These will be conducted with as-irradiated materials to determine the bending stiffness and failure energy for fueled cladding and survivability of the

fueled cladding to energy-limited impact loads. If the ANL tests determine that radial hydride formation results in significant cladding degradation, then these tests will be repeated on fuel segments subjected to RHT conditions that promote radial hydride formation.

The sequence of testing with regard to cladding alloy type has been determined based on several factors: fraction of cladding-alloy type in spent-fuel pools and dry casks, amount of hydrogen pickup at high burnup, and material availability. PWR Zry-4 has been selected as the first alloy to study because of the relatively high number of these rods in storage and the high hydrogen pickup (600-800 wppm) at high-burnup. The 15×15-assembly cladding is from fuel rods irradiated to 63-67 GWd/MTU in a H. B. Robinson Reactor. In order for ANL to continue its Zry-4 study, Robinson rod segments must be shipped to ORNL for sectioning, defueling and shipment back to ANL. 17×17 assembly ZIRLO has been selected as the second alloy to study because of its high hydrogen content (500-700 wppm) at high burnup and its availability at ANL. The cladding is from fuel irradiated to 70 GWd/MTU in a North Anna Reactor. In terms of fraction of SNF in storage, it would have been logical to select BWR Zry-2 as the second alloy to study. However, at ANL the high-burnup (56 GWd/MTU) 9×9-assembly Zry-2 cladding from Limerick fuel rods has only ≈70-wppm hydrogen. GNF has higher burnup Limerick fuel that could be made available to this program. If the cladding contained 200-300 wppm hydrogen, then it would be worth testing. M5 is ranked fourth in priority because of its low hydrogen content (≤120 wppm) at high burnup. 17×17 assembly M5 cladding (defueled) irradiated to 68-72 GWd/MTU in a North Anna Reactor is available at ANL.

1. Introduction

1.1 Background

Pressurized (PWR) and Boiling (BWR) water reactor fuels are licensed to operate up to 62 GWd/MTU (rod axial-average) burnup. For conventional and low-tin Zircaloy-4 (Zry-4) PWR cladding, such operation can result in waterside corrosion (oxide) layer thicknesses up to 100 μm and hydrogen pickups up to 600-800 wppm. The oxide layer causes a small decrease in cladding wall thickness (e.g., ≤ 0.06 mm from an initial wall thickness of 0.67-0.76 mm for 15 \times 15 Zry-4 and from an initial wall thickness of ≈ 0.57 -mm for 17 \times 17 Zry-4) and load-bearing metal. In unirradiated cladding, hydrogen content beyond the solubility limit (≈ 70 -130 wppm at 300-350°C) precipitates out as zirconium hydrides. In the irradiated condition, higher hydrogen contents can be accommodated before hydride precipitation. The excess hydrogen beyond the thermodynamic limit may be due to hydrogen trapped in irradiation defects in the cladding. During cooling to room temperature, the trapped hydrogen may remain trapped and may not precipitate as hydrides. Zry-4 in the cold-worked-and-stress-relieved (CWSR) condition is textured to precipitate excess hydrogen as platelets oriented in the circumferential direction. This hydride orientation is less embrittling than hydrides oriented in the radial direction or in directions within $\pm 40^\circ$ of the radial direction. As shown in Fig. 1, the hydride density in high-burnup Zry-4 cladding is greater during reactor operation near the coolant side of the cladding, relative to the hotter middle and inner cladding regions. The combination of radiation-induced hardening and hydrides causes an increase in strength and a decrease in ductility of the cladding. Although radiation-induced hardening is expected to saturate within a couple of reactor cycles, increased burnup, or more exactly fast-neutron fluence, can result in additional hardening due to local changes in precipitate size and chemical composition. Hydrogen pickup increases with burnup, or more exactly with extent of waterside corrosion, thereby causing cladding ductility and failure energy to decrease with burnup. Zry-4, with a significant fraction of radial hydrides, is expected to have a brittle-to-ductile transition temperature in the range of 150-350°C.

ZIRLO and M5 are advanced PWR cladding alloys that exhibit significantly better corrosion resistance than Zry-4 under the same operating conditions. However, under conditions of higher cladding heat flux and temperature at the cladding-coolant boundary, high-burnup ZIRLO can develop a peak corrosion layer thickness of 80 μm and peak hydrogen content in the range of 600-800 wppm. Defueled cladding segments at ANL for one of the North Anna high-burnup fuel rods have measured hydrogen contents of 590-670 wppm at corrosion-layer thicknesses of 40-45 μm . High-burnup M5 exhibits low corrosion-layer thickness (< 25 μm) and low hydrogen pickup (< 120 wppm) under current operating conditions. Because of higher hydrogen pickup, a higher priority is placed on ZIRLO than M5 testing in the ANL program.

BWRs use Zry-2 cladding with an inner-wall liner of low-alloy Zr – about 10% of the wall thickness. The coolant temperature is relatively constant (288°C) along the length of these rods and lower than PWR coolant temperatures. High-burnup BWR rods exhibit peak corrosion layers in the range of 20-30 μm . Although the peak corrosion layer is comparable to that of M5, the peak hydrogen content is higher -- in the range of 200-300 wppm, depending on the local operating conditions (e.g., heat flux and cladding temperature at the cladding-coolant surface).

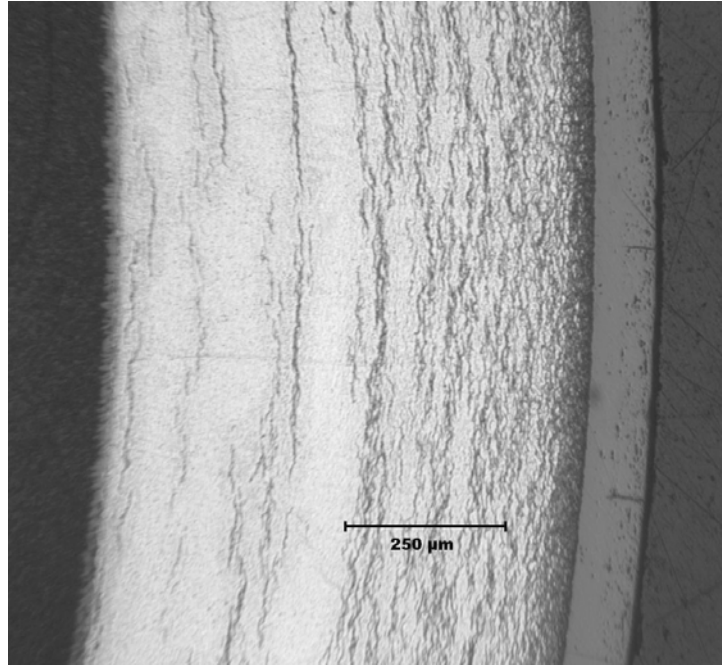


Fig. 1. Hydride distribution in H. B. Robinson PWR fuel rod A02 (67 GWd/MTU) cladding at ≈ 0.7 m above the fuel midplane. Corrosion layer (right) is ≈ 100 μm and hydrogen content is ≈ 750 wppm. Hydrides increase in density from left (fuel side) to right (coolant side).

Unlike PWR cladding, high-burnup BWR cladding does exhibit evidence of radial hydride formation during in-reactor cooling and prior to drying and storage operations. The ductile-to-brittle transition temperature for BWR cladding with a significant fraction of radial hydrides is estimated to be in the range of 150-250°C.

The term “ductility” is used in this work to refer to the extent to which the cladding can deform beyond the elastic limit prior to failure. This inelastic deformation can be due to plasticity and/or microcracking. The degree of cladding ductility depends on the material condition, temperature, loading and deformation modes, loading and deformation rates, loading and deformation history, and the extent of flaws that may be present on the outer (coolant) and inner (fuel) surfaces of the cladding prior to testing. Typical loading modes considered in modeling the behavior of PWR cladding during normal operation are external coolant pressure (≈ 15.5 MPa), internal gas pressure due to He fill gas and released fission gases (< 15.5 MPa for most fuel rods, < 20 MPa for a limited number of rods), and fuel-cladding mechanical interaction due to creep-down of the cladding onto the fuel followed by radial expansion of the fuel.

After discharge from the reactor, the spent nuclear fuel rods are stored in a pool at a temperature that is typically $< 50^\circ\text{C}$. This is a relatively benign environment for intact rods. Although the external pressure on the rods is reduced to ≈ 0.1 MPa, the internal gas pressure also decreases with decreasing temperature, and fuel-cladding mechanical interaction decreases to essentially zero due to differential thermal contraction during cooling.

As the spent fuel pools have limited storage capacity, nuclear power utilities are licensed to store fuel in dry storage systems located on pads at the power plant sites. These large storage systems maintain an inert atmosphere (helium) around the spent nuclear fuel. Some systems are licensed for storage only, while others are licensed for storage-and-transport. Storage system licenses were originally issued for low-burnup (≤ 45 GWd/MTU) fuel and for ≤ 20 years. Presently, systems are being licensed for storing commercial fuel with burnup up to the levels licensed by the Office of Nuclear Reactor Regulation, i.e., peak rod-average burnup of 62 GWd/MTU, and licenses extending the storage time to 60 years have been granted. However, there are no generic acceptance criteria for transportation of spent fuel with burnups > 45 GWd/MTU.

1.2 Discussion

Transfer of spent fuel from wet to dry storage requires handling and drying operations. Drying of low burnup spent fuel has relied on the application of a vacuum to remove the water from the cavity (cask or canister) holding the spent fuel. Peak cladding temperatures and times at elevated temperature vary from vendor-to-vendor for these operations. For low-burnup PWR fuel currently in storage, maximum drying-transfer temperatures ranged from ≈ 200 to $\approx 500^\circ\text{C}$ and vacuum drying times ranged from a few days to several weeks. During these operations, partial annealing of radiation hardening may occur, and some of the hydrides in the cladding will go in solution (e.g., ≈ 200 wppm at 400°C) into the solid zirconium matrix. During cooling under low cladding hoop stress, the hydrogen in solution re-precipitates out as circumferential hydrides with a more uniform distribution across the radius of the cladding (see Fig. 2). Annealing and hydride redistribution should result in a decrease in hardening and an increase in ductility. For example, radiation damage and hydriding (see Fig. 1) result in an increase in axial strength properties [RT yield strength (YS) = 600 MPa \rightarrow 770 MPa, RT ultimate tensile strength (UTS) = 770 MPa \rightarrow 950 MPa] and a decrease in ductility [RT uniform elongation (UE) = 6% \rightarrow 3%, total elongation (TE) = 14% \rightarrow 4%], relative to the as-fabricated (fresh) cladding. High-burnup Zry-4 samples from the H. B. Robinson PWR were heated stress-free to 420°C for 72 h. This treatment resulted in a 75% recovery of radiation hardening in the Zry-4 cladding, based on RT microhardness measurements. Thus, the room-temperature value of YS for the Robinson cladding was estimated to decrease to ≈ 640 MPa after 72 hours at 420°C . This reduction in radiation embrittlement, along with the more uniformly distributed hydrides, should result in an increase in ductility. The behavior of high-burnup cladding following heating to $\leq 400^\circ\text{C}$, holding at $\leq 400^\circ\text{C}$, and cooling under stress will be investigated in this program.

If cooling after drying and back-filling, as well as cooling during storage, occurs under a high enough initial hoop stress (e.g., 120 MPa at 400°C) and slow enough rate (e.g., $< 5^\circ\text{C/h}$), some of the hydrogen in solution may precipitate out in the radial or near-radial ($\pm 40^\circ$ from radius) direction. Figure 3 shows that nearly 100% of the hydrogen in the Robinson cladding precipitated out in the radial direction following cooling from 400°C to 200°C at 190-MPa engineering hoop stress. As the measured hydrogen content near this cross-section is 320 wppm, the results also suggest that the apparent¹ hydrogen solubility may be higher in high-burnup Zry-4 cladding than it is in non-irradiated Zry-4 tubing and sheet.

¹ The apparent solubility is defined as the sum of (1) hydrogen at a concentration dictated by thermodynamic considerations, and (2) hydrogen trapped in irradiation defects (especially a- and c-dislocation loops).

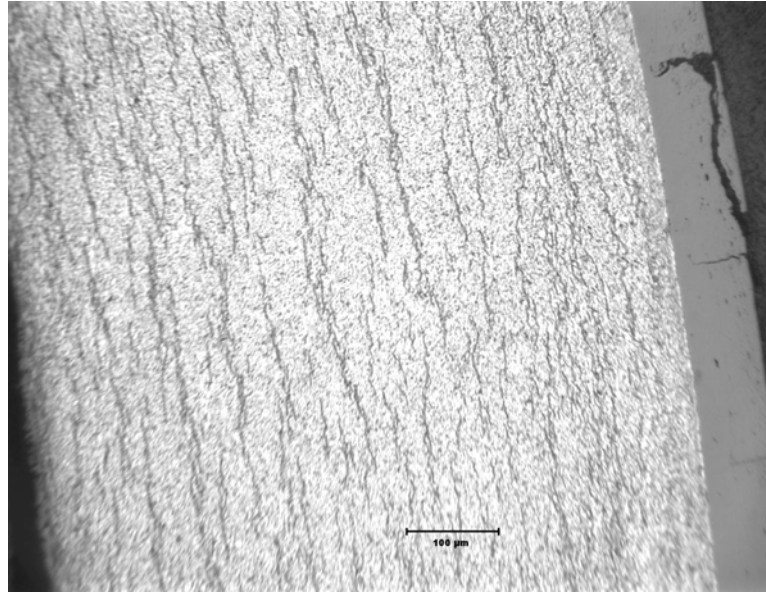


Fig. 2. Uniform, circumferential hydride distribution in H. B. Robinson PWR fuel rod A02 (67 GWd/MTU) cladding from fuel midplane (≈ 550 wppm H) after stress-free annealing at 420°C for 72 hours. Decrease in microhardness suggests $\approx 75\%$ recovery of radiation-induced damage.

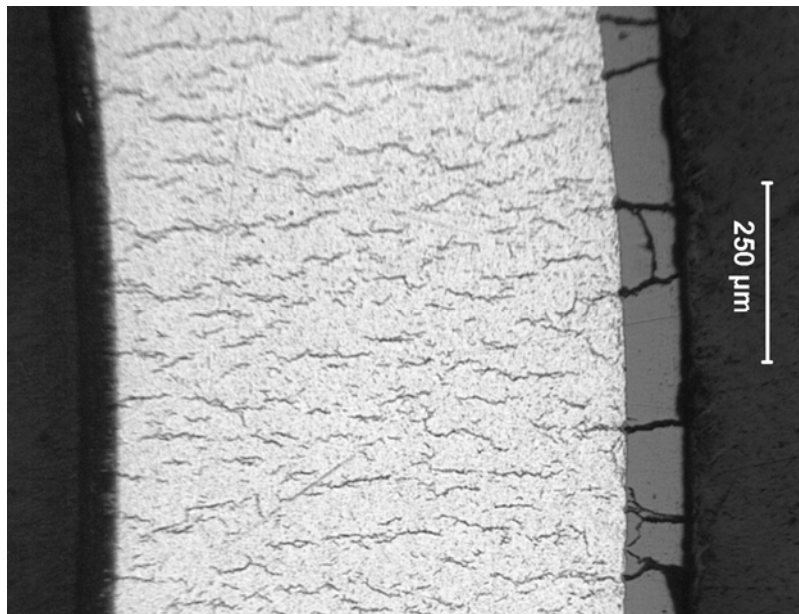


Fig. 3. Radial hydrides formed in Robinson PWR fuel rod A02 (67 GWd/MTU) cladding at ≈ 0.4 m above the midplane after cooling from 400°C to 205°C at $1^\circ\text{C}/\text{minute}$ and 190 MPa hoop stress, following 101 days of thermal creep to $\approx 4\%$ strain at 400°C and 190 MPa. Note: sample lost ≈ 350 wppm H due to axial diffusion to end caps, giving a hydrogen content of ≈ 320 wppm during cooling under stress.

Extensive formation of radial hydrides can significantly reduce the ductility and impact resistance of high-burnup cladding. This would be particularly true for loads that induce hoop tensile stresses in the cladding, as these stresses would be perpendicular to the radial hydrides. At the lower temperatures (e.g., 150-250°C) anticipated at the end of dry cask storage, the radial hydrides may act as brittle sites or pathways for crack propagation across the wall of the cladding. These cracks can grow axially, as well, and may represent a failure mechanism for fuel dispersal. The extent of such dispersal would depend on the loading and axial extent of the crack(s). Also, because of the difference in density between Zry-4 and the hydrides, stresses at the Zry-4/hydride interfaces could be enhanced. These interfaces may be more vulnerable to crack propagation than the hydrides themselves.

In addition to the possible formation of non-circumferential hydrides during cooling from drying and long-term storage, the cladding will experience some creep-out due to the higher internal pressure anticipated for high-burnup fuel. Although the magnitude of the creep strain is limited by the continued cooling and gas-pressure decrease with time during cask storage, creep-out of the cladding will increase the fuel-rod internal volume, decrease the internal pressure, and reduce the cladding hoop stress with time beyond the reduction that would occur with the decrease in temperature with time. Cladding thermal creep during early handling, drying and storage at 350-400°C could decrease, or eliminate, radial hydride precipitation during long-time cooling.

High-burnup cladding, which experienced some radial hydride formation and perhaps some thermal creep, would be most vulnerable to brittle failure at the end of dry-cask storage when the cladding temperature would be at its lowest value. Such cladding could experience brittle failure, as well as some fuel dispersal, during post-storage handling and transportation operations, particularly under accident conditions (e.g., cask and/or assembly drop). Thus, in assessing the structural integrity of the cladding in transfer operations from cask storage to a repository, it is important to assess the effects of the whole history of the cladding during wet-to-dry transfer, including drying and backfilling operations, transfer to the storage pad, and long-term storage. Of all these steps, drying operations involving vacuum could have the highest potential for generating both high temperatures and stresses, and thus lead to the most damaging effect on cladding integrity.

2. Licensing Issues Requiring Additional Data for High-Burnup Cladding

2.1 NRC-NMSS

The Division of Spent Fuel Storage and Transport (DSFST, formerly SFPO) periodically issues Interim Staff Guidance (ISG) for evaluating license applications for dry storage and transportation systems. ISG-11, Rev. 3 (November 2003) addresses cladding issues associated with dry storage of spent fuel of any burnup based on regulations in 10 CFR Part 72. To a lesser extent, issues associated with transportation (10 CFR Part 71) are also mentioned.

For low-burnup fuel (≤ 45 GWd/MTU), ISG-11 (Rev. 3) provides the option for peak cladding temperatures higher than 400°C for normal conditions of storage and for short-term operations prior to storage (drying, backfilling, transfer to storage pad) as long as the cladding hoop stress remains at ≤ 90 MPa. This stress limit is based on a very mixed set of data, which includes data for prehydrided-nonirradiated cladding and some low-burnup cladding under a wide range of cooling rates, most of which are very fast relative to anticipated cooling rates during drying, transfer and storage. Also, parameters that may be important in determining the radial hydride density and effective continuity across the cladding wall (e.g., total hydrogen content and apparent hydrogen solubility, which both increase with burnup) vary considerably from data set to data set. Figure 4 shows a selective compilation of data in terms of initial temperature and stress level prior to cooling. Most, if not all, of the tests used to generate the data were conducted with cooling under constant stress, which enhances radial hydride formation relative to SNF rod conditions during storage. These data were used by NMSS-SFPO (now DSFST) to set the 90-MPa limit at a peak temperature of 400°C for low-burnup fuel. However, applicants are allowed to go as high as 570°C for short-term operations involving low-burnup fuel as long as the hoop stress is limited to 90 MPa. In addition, the number of thermal cycles during these short-term operations is limited to <10 if the temperature change during cycling is $>65^{\circ}\text{C}$. For short-term accidents and off-normal conditions, the cladding temperature is limited to 570°C , based on creep-rupture life of low-burnup Zry-4. While such a limit may protect against short-time creep rupture, it is not clear to what degree this high temperature (followed by cooling) would degrade the cladding.

For high-burnup (45-62 GWd/MTU) cladding, a peak cladding temperature of 400°C is specified during drying, transfer, and storage, but no stress limit has yet been imposed. A major purpose of the proposed tests in the ANL high-burnup SNF program is to generate data correlating drying temperature ($\leq 400^{\circ}\text{C}$) and stress conditions that would lead to radial hydride formation and potential cladding degradation during long-time cooling.

In consideration of anticipated loads on the cladding during storage and transport, NRC is sponsoring work at ANL to determine axial tensile properties, drying conditions for radial hydride formation, and the effects of radial hydrides on the performance of high-burnup cladding. Axial tensile properties and failure limits are important for the analysis of vibration-induced bending loads during normal transport and fuel assembly retrieval, as well as during seismic events and handling-transport accidents. Given the uncertainty in the T vs. σ curve for radial hydride precipitation, the purpose of the ANL study is to better determine conditions for, and effects of, radial hydride formation. In addition, in a User Need memo (March 5, 2004), NRC-

NMSS has requested impact data on high-burnup Zry-4 cladding, as well as on advanced ZIRLO and M5 cladding alloys, at temperatures of 150°C, 350°C and 400°C. The data needs are for as-irradiated cladding and cladding subjected to drying conditions. High-burnup ZIRLO and M5 will be subjected in this program to the same axial tensile tests, ring-compression tests and crush-impact tests as Zry-4 in the as-irradiated and simulated post-drying state to determine stresses at peak drying temperatures that lead to significant degradation of ductility and failure energy.

Fracture toughness tests are not included in the NMSS data needs or in this test plan. Given the current state-of-the-art in fracture toughness testing of relatively thin-walled tubing, such tests only give information regarding axial crack growth rates and fracture toughness under hoop tensile loading for samples with fabricated pre-test axial cracks. The data are applicable only for this loading mode (e.g., fuel-cladding mechanical interaction from fuel pellet expansion). They are not applicable for crack propagation across the wall of the cladding due to a pre-test flaw (e.g., inner-surface cladding flaw from pellet-clad interaction during normal operation).

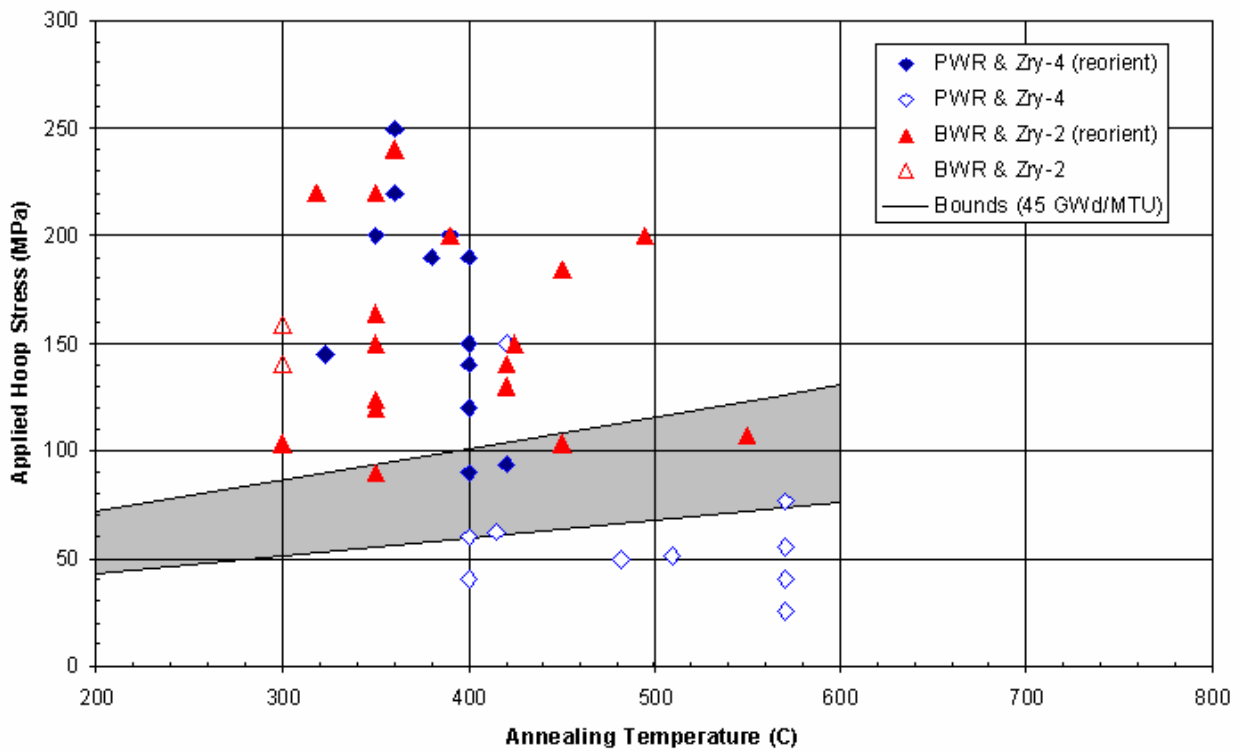


Fig. 4. NMSS-SFPO data compilation on stress-temperature conditions for radial hydride formation (from R.E. Einziger and C. Brown presentation at ANL/NRC Program Review, Aug. 24, 2005).

2.2 DOE-RW Office of National Transportation (ONT) Data Needs

As an applicant for the permanent repository license, DOE-RW has extensive needs for high-burnup fuel and cladding data. The high-burnup cladding data needed by DOE-RW-ONT for justification of spent fuel transport to the repository are addressed in this section. Regulations regarding transport of casks containing nuclear materials are specified in 10 CFR Part 71. Transport by truck or rail would induce dynamic loads that would cause vibration of the rods within the cask. Currently, rail transport is planned to the greatest possible extent. If the package were transported in a vertical position, the primary response of the fuel rods would be vibratory bending along the length of the rods, which would cause alternating axial tension-compression bending stresses and possible fatigue concerns. If the package were transported in a horizontal position, alternating axial bending stresses would be induced, along with possible impact between the cladding and the grid spacers. As the package's exterior and internals are designed for such dynamic loadings, it is unlikely that fuel-rod failure would occur under normal transportation loads unless the cladding were highly embrittled and flawed (e.g. large radial cracks at the fuel-cladding interface).

Accidents involving cask end-drop, edge-drop and side-drop – 1-foot drop specified for normal transportation in 71.55 (d) and 30-foot drop specified for severe accidents in 71.55 (b) – would induce larger impact loads than rail transportation loads. Figure 5 is a schematic showing the predicted response of a fuel rod assembly to cask end-drop and side-drop accidents (from Sanders et al., SAND90-2406, 1992). The fuel rod would experience more significant bending deformation and axial stress, as well as local impact with the grid spacers and possibly the wall of the cask-internal basket, for the side-drop accident. In order to predict the deformation response of the fuel rod, tensile properties for high-burnup cladding are needed. In addition, ductility limits and impact-resistance limits are needed.

Basically, the data needs for DOE-RW-ONT and NRC-DSFST are the same with regard to fuel assembly response to normal and accident transportation loads. From a practical perspective, DOE-RW-ONT needs to work with the cask vendor in convincing NRC-DSFST and -NMSS that the transportation casks they are purchasing for high-burnup fuel satisfy the requirements in 10 CFR 71. They also need to assure that the geometric form of the transportation package contents (basket, fuel assemblies and rods) would not be substantially altered under normal conditions as bounded by the one-foot drop. Data and analyses are needed to support the criticality evaluation to be performed under accident conditions, as bounded by the 30-foot drop, which, in turn, may require an evaluation of the configuration of the package contents after a hypothetical accident. Additional issues beyond the current scope of this program are cask-drop and assembly-drop accidents during handling and transfer at the repository. However, the data generated in this program are applicable to repository handling operations as well.

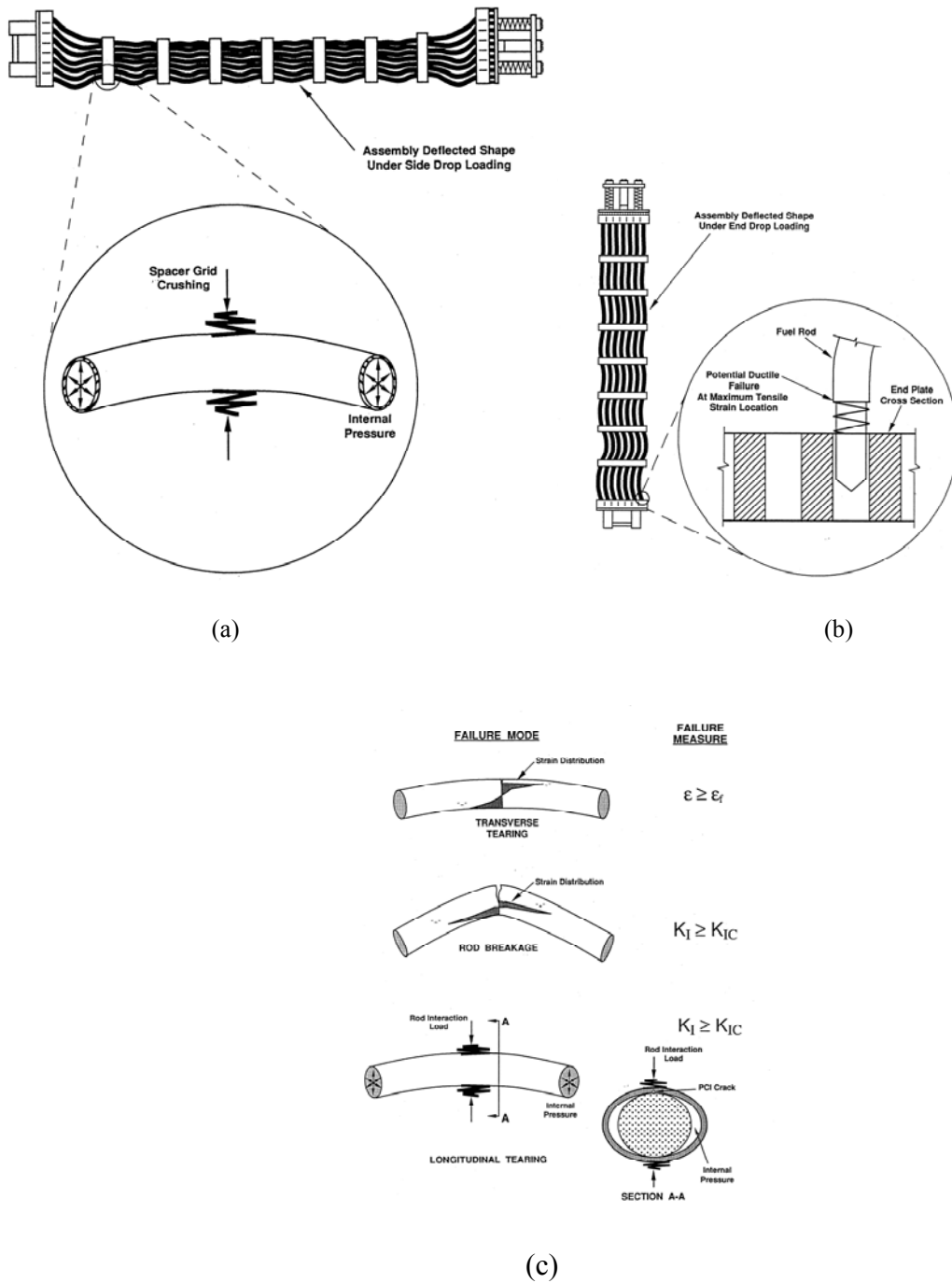


Fig. 5. Examples of deformation and loading during postulated handling and transportation accidents showing (a) crushing or impact, (b) bending loads and (c) some proposed fracture criteria [Reference: T. Sanders et al., "A Method for Determining the Spent-Fuel Contribution to Transport Cask Containment Requirements," SAND90-2406/TTC-1019/UC-820, November 1992].

3. ANL Test Program

The ANL high-burnup test program makes use of the cladding from high-burnup PWR rods from the H.B. Robinson reactor. These rods are described in the EPRI Report 1001558 (O. Ozer, "Design, Operation, and Performance Data for High-Burnup PWR Fuel from the H. B. Robinson Plant for Use in the NRC Experimental Program at Argonne National Laboratory," May 2001). ANL characterization results for Robinson rod A02 can be found in the NSRC-2002 and NSRC-2003 papers presented by H. Tsai and published in the Proceedings. The operating conditions and characterization of direct relevance to mechanical properties and limits are the fast ($E > 1$ MeV) neutron fluence (14×10^{25} n/m²) and the hydrogen content (≈ 400 to ≈ 800 wppm) in the uniform flux region along the rod (excluding cladding under grid spacers).

The specific tests relevant to the SNF program are: high-strain-rate axial tensile tests (RT to 400°C, with emphasis on 150° and 250°); high-strain rate ring-compression screening tests for cladding samples ranging from the as-irradiated condition to varying degrees of radial hydride formation induced by cooling under stress; and crush-impact tests with sibling RHT samples. Annealing tests on non-stressed samples have been completed and are not included in this test plan (see Fig. 2 for example of results).

3.1 Axial Tensile Properties

Axial tensile specimens are 76-mm-long with a gauge length of 25 mm. A double gauge is machined by EDM such that each gauge has a width of 2.5 mm. Figure 6 shows the EDM instrumentation and control unit outside Irradiated Materials Laboratory (IML) Cell#3. Figure 7 shows the EDM inside Cell#3, and Fig. 8 shows an axial tensile sample being fabricated by the electrical discharge of the wire. An Instron 8511 servo-hydraulic machine is used to perform the axial tensile tests. Figure 9 shows the Instron prior to insertion into the glove box and the set of two glove boxes that now house the Instron, the microhardness tester, the oxide removal device, the pin-hole-drill device, a lathe, sample cleaning equipment and imaging instrumentation. Based on crosshead displacement rate normalized to the gauge length, the two strain rates used in testing are 0.1%/s and 100%/s. Test temperatures are in the range of room-temperature (RT) to 400°C for the SNF program. Because of partial annealing and hydride redistribution which occur during drying operations, these properties represent an upper-bound with regard to strength (YS and UTS) and a lower-bound with regard to ductility (UE and TE). In addition to providing the standard engineering properties, these tests are designed to generate plastic stress-strain data for modeling.

In this program, axial tensile properties of archival (or near-archival) and irradiated cladding are determined to allow direct comparison. For the PWR Robinson cladding, the archival properties are the tensile strengths and plastic ductility parameters for cold-worked and stress-relieved Zircaloy-4. Based on the vendor-supplied tensile properties for the as-fabricated material (15×15 archive tubing and 15×15 low-tin tubing), the expected yield strength (YS), ultimate tensile strength (UTS) and total elongation (TE) are 550-580 MPa, 725-760 MPa, and



Fig. 6. Photograph of the EDM instrumentation and control unit outside of IML Cell#3, in which the EDM is located.

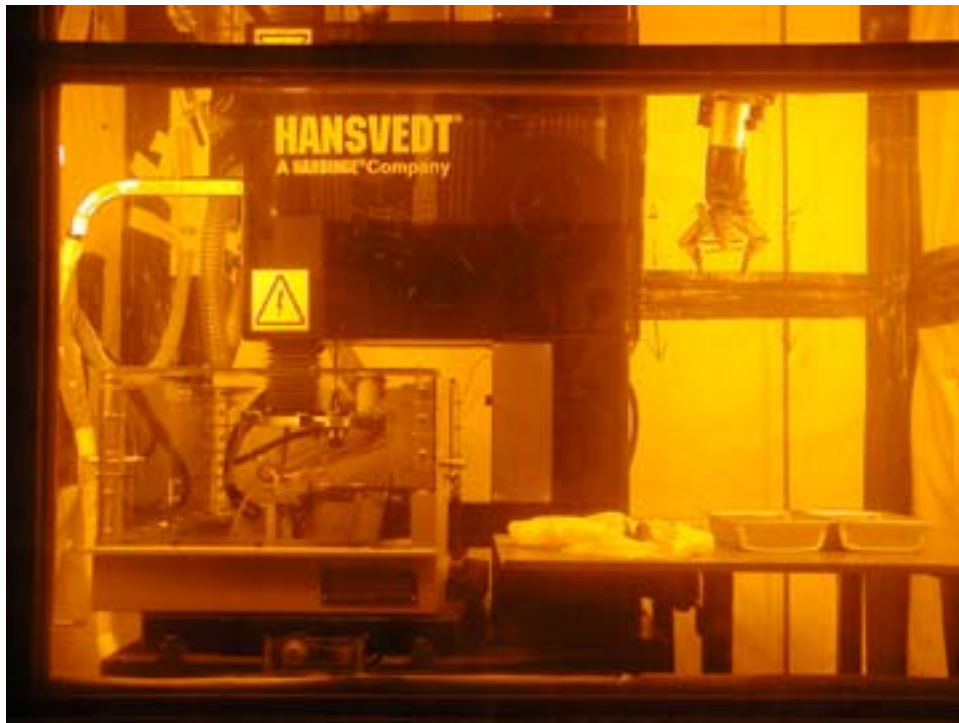


Fig. 7. New EDM inside IML Cell#3.



Fig. 8. Close-up view of fabricating axial-tensile-sample gauge section using wire electrical discharge for fine cutting.

20-22%, respectively, at room temperature, and 320-360 MPa, 400-440 MPa, and 22-28%, respectively, at 382°C.

Table 1 gives the test matrix for determining the axial tensile properties of irradiated H.B. Robinson Zircaloy-4 and unirradiated Zry-4 cladding. The reference strain rate for these tests is 100%/s. A limited number of tests are being conducted at 0.1%/s and 25°C, 150°C and 400°C to determine strain rate sensitivity. Axial tensile tests have been completed at 25°C and 400°C at 0.1%/s and at 400°C at 100%/s with high-burnup Zry-4 samples. Additional testing has been delayed until ANL can ship HBR fueled Zry-4 segments to ORNL, and defueled cladding segments can be shipped back to ANL. The executed-and-signed contract between ANL and ORNL includes this work.



**Instron 8511
Prior to Installation**



**Instron 8511 in
Glovebox Containment**

**Microhardness
Indenter**

**Optical
Microscope**

Fig. 9. Instron 8511 test machine prior to installation into large glove box and both the large and small glove boxes in the IML

Table 1 Matrix for Axial Tensile Tests of the H.B. Robinson High-Burnup PWR Zircaloy-4 Cladding Specimens; TBC = To Be Completed.

Material	Fuel Rod ID No.	Grid Span	Strain Rate, %/s	T, °C	No. of Tests	Status
H.B. Robinson Irradiated Zry-4	A02	4	0.1, 100	25	2, 1	2 Completed
	R01	4-5	0.1, 100*	150	1, 1	TBC
	B01	5	100	250	1	TBC
	A02	5	0.1, 100	400	1, 1	2 Completed
Unirradiated Zry-4 10.77-mm OD 0.76-mm wall	---	---	0.1, 100	25	1, 1	Completed
	---	---	0.1, 100	200	1, 1	Completed
	---	---	0.1, 100	300	1, 1	Completed
	---	---	0.1, 100	350	1, 1	Completed
	---	---	0.1, 100	400	1, 1	Completed

*This test is to be repeated with a sibling sample preconditioned at 400°C for 3 days and slow-cooled (5°C/h) under decreasing stress from 150 MPa at 400°C.

Proprietary data are most likely available to NRC for the axial tensile properties of as-fabricated and high-burnup ZIRLO and M5 cladding. Generally, company-proprietary data for as-fabricated cladding are generated by the tubing manufacturer at RT and 350-380°C to satisfy design specifications. Tensile data are also generated for high-burnup PWR cladding at $\geq 280^\circ\text{C}$ for determining behavior under normal operating conditions (low strain rate) and RIA conditions (high-strain rate). Because of the limited number of high-burnup ZIRLO (8) and M5 (3) samples currently available at ANL for SNF testing, it is prudent to initiate tensile testing at 100%/s strain-rate and 150°C. Additional defueled high-burnup M5 samples can be obtained through the ANL contract with ORNL. Additional defueled high-burnup ZIRLO samples would have to be obtained from Studsvik in the near-term and possibly from ORNL in the longer term if EPRI supplies high-burnup ZIRLO rods for the NRC LOCA and SNF program. The test matrix for ZIRLO and M5 is described in Table 2.

Table 2 Matrix for Axial Tensile Tests of High-Burnup PWR ZIRLO and M5 Cladding Irradiated in the North Anna Reactor; TBC = to be completed and TBD = to be determined; tests in bold are for cladding samples that are currently at ANL

Material	Corrosion Level, μm	H wppm	Strain Rate, %/s	T, $^{\circ}\text{C}$	Status
High-Burnup ZIRLO	TBD	TBD	100	25	TBC
	TBD	TBD	0.1	150	TBC
	38-42	TBD	100*	150	TBC
	TBD	TBD	100	250	TBC
High-Burnup M5	≤ 20	TBD	100	25	TBC
	≤ 20	TBD	0.1	150	TBC
	≤ 20	TBD	100*	150	TBC
	≤ 20	TBD	100	250	TBC

*This test is to be repeated with a sibling sample preconditioned at 400°C for 3 days and slow-cooled (5°C/h) under decreasing stress from 150 MPa at 400°C.

Sample characterization and preparation for high-burnup ZIRLO and M5 cladding present new challenges as compared to the high-burnup Zry-4 samples already prepared and tested. Preparation of characterization samples, characterization by optical microscopy, oxide removal (required for EDM-cutting of gauge sections) from the middle 50 mm of the tensile samples and pin-supported end-fixturing operations were conducted in the AGHCF up through June 2005. As this facility is no longer available, these operations are now conducted in DL-114 and IML glove boxes and IML Cell #3 (EDM cutting). The oxide removal capability and the drilling and pin-loading of end-caps have been established in the Instron glove box (G/B#1) in the IML. Prior to starting the DL-114 upgrade, glove boxes with leaded-glass windows (to reduce worker exposure) were available for LECO hydrogen (G/B-13 in Fig. 10) and LECO oxygen (G/B-162 in Fig. 10) determination. Two of the remaining glove boxes in DL-114 have been reinforced to handle the weight of leaded-glass windows that needed to be installed on two sides of each glove box and lead blankets for the top of the glove boxes. Figure 10 is a schematic of the glove box arrangement in DL-114. G/B-9 is used for cleaning, cutting, microbalance measurements and met mount preparation. A new optical microscope has been installed in refurbished/leaded-glass-shielded G/B-153 and used for metallography of high-burnup samples to determine corrosion layer thickness and hydride morphology. G/B-163 is being refurbished for SNF rodlet fabrication and RHT. The laser welder shown in Fig. 10 is used to pressurize and seal non-irradiated rodlets for SNF testing. Most of this equipment will also be used for pressurization-and-welding high-burnup cladding rodlets for the RHT to be performed in G/B-163.

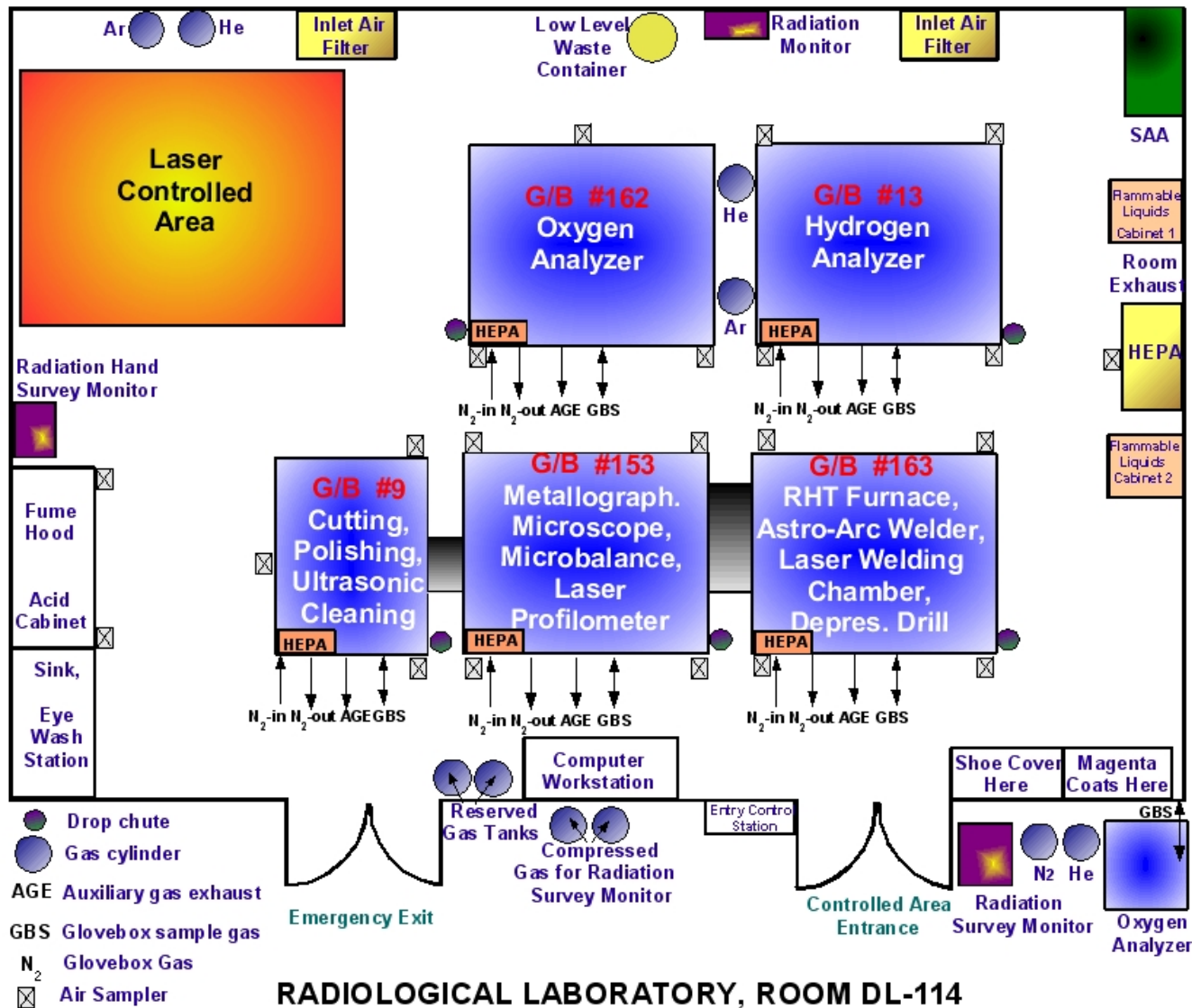


Fig. 10. DL-114 glove boxes for high-burnup cladding sample preparation, characterization and testing.

In addition to the challenges in re-establishing capabilities lost with the closure of the AGHCF to programmatic work, high-burnup ZIRLO and M5 cladding samples emit very high beta dose rates and high gamma doses rate as compared to HBR Zry-4. For glove box work, this requires new procedures and personal protective equipment to minimize worker extremity dose. The ANL administrative limit for extremity dose due to gamma radiation is 1 rem/month/worker. Although DOE does not put a limit on beta-dose accumulation, the observation that it is present requires that action be taken to minimize worker exposure. For the 80-mm defueled ZIRLO and M5 cladding segments received from Studsvik and the 76-mm-long M5 segments received from BWXT, extensive dose rate readings have been measured on-contact, at 8 cm from the axial midplane, at 8 cm from the ends of the samples, and at 30 cm from the axial midplane. Measured on-contact dose rates were found to be unreliable and difficult to extrapolate to positions away from the samples: high variability in gamma dose rate along the sample (e.g., 5-15 R/h) and beta-gamma dose rates that pegged the detector at > 200 R/h. The readings at 8 cm from the axial midplane of the samples were found to be reliable, repeatable and within the calibration range of the detector. These values are summarized below:

North Anna ZIRLO (70 GWd/MTU) defueled by Studsvik: 0.6-2.0 R/h γ , 6-11 R/h β - γ

Ringhals M5 (63 GWd/MTU) defueled by Studsvik: 1.2-1.5 R/h γ , 16-20 R/h β - γ

North Anna M5 (70 GWd/MTU) defueled by Studsvik: 2.1-4.1 R/h γ , 44-69 R/h β - γ

In addition to possible differences in quality and extent of defueling, the dose rate readings appear to correlate directly with local burnup and reactor discharge rate: North Anna ZIRLO rod (60-76 GWd/MTU local burnup; March 12, 2001 reactor discharge); Ringhals M5 (69 GWd/MTU local burnup; July 31, 2003 reactor discharge); and North Anna M5 (71-76 GWd/MTU local burnup; and May 2, 2004 reactor discharge).

Based on the sectioning and characterization work performed in DL-114, ANL Health Physics and the NE Division ALARA and Safety Committees have approved doing glove box work with samples that have dose rates of 2 R/h gamma @ 8 cm and 23 R/h beta-gamma @ 8 cm. To qualify the North Anna M5, wire-brushing of the cladding inner-surface, followed by possible nitric acid cleaning, is required to reduce the beta-gamma dose rate to currently acceptable levels. The source term limits can also be increased somewhat by demonstrating that routine glove-box work can be performed on such samples without excessive worker extremity dose pickup.

3.2 Thermal Creep Test Results

Thermal creep tests have been conducted using samples from intermediate-burnup Surry rod cladding following 15 years of dry-cask storage and samples from as-irradiated, high-burnup H. B. Robinson cladding. Results of these creep tests have been presented by Tsai at NSRC-2003 and by Billone at the 14th International Symposium on Zirconium in the Nuclear Industry (Stockholm, June 14-17, 2004; published in JAI, Jan. 2006, Vol. 3, No. 1, Paper JAI12425). Although no additional creep tests are planned, the results are presented in Table 3 to aid in planning for radial-hydrided treatment hold times at 400°C and because three of the samples were cooled under constant gas pressure at $\approx 1^\circ\text{C}/\text{min}$ to determine hydride morphology. Two of them (HBR-C15 and S-C6) are used in this program to determine RT ring-compression ductility of radial-hydride treated samples. The data suggest that thermal creep for high-burnup Zry-4 should be $<0.1\%$ at 400°C and <190 MPa for a 72-hour hold time.

Table 3 Thermal Creep Test Results for H.B. Robinson (HBR) High-burnup PWR Zry-4 Cladding Specimens (600-750 wppm initial hydrogen content) and for Intermediate-burnup Surry (S) PWR Cladding (250-300 wppm initial hydrogen content).

Sample ID	T °C	Hoop Stress ^a MPa	Time hours	Average ^b Hoop Strain %	Comments
HBR-C14	400	190	72 2427	0.03 3.7	
HBR-C15	400	190	48 2439	0.07 3.5	Midplane H content decreased from ≈ 670 wppm to 320 wppm during creep tests; final cooling at $1^\circ\text{C}/\text{min}$. under pressure; 8-mm rings sectioned
HBR-C17	380	220	404	0.12	
HBR-C16	380	190	404	0.11	
S-C9	400	190	49 1873	0.08 1.04	---
S-2C9	400	160	44 286	0.07 0.22	---
S-C8	380	220	2180	1.10	---
S-C6	380	190	2348	0.35	Midplane H content decreased from ≈ 250 wppm to 130 wppm during creep tests; final cooling at $1^\circ\text{C}/\text{min}$. under pressure; 8-mm ring sectioned
S-C3	360	220	3305	0.22	Final cooling under full pressure

^aWall-averaged engineering hoop strain (does not include wall thinning)

^bWall average and axially average of data within ± 15 mm of specimen midplane

3.3 Cladding Degradation due to Hydride Reorientation: Ring-Compression Screening Tests

There are four phases to this program: (1) prehydriding cladding alloys; (2) preconditioning to simulate the thermal effects of drying, transfer and storage; (3) measuring ring-compression ductility and failure energy vs. preconditioning temperature-stress; and (4) determining hydride morphology as a function of preconditioning temperature and stress histories.

3.3.1 Prehydriding cladding alloys

Both radiation hardening and hydrogen pickup can decrease the failure ductility and energy of cladding alloys during in-reactor operation. However, during drying-transfer-storage-transport, possible reorientation of hydrides formed during cooling can lead to the most severe degradation of cladding behavior. Prehydrided cladding offers a reasonable and practical surrogate for hydrogen behavior in high-burnup cladding. A range of hydrogen contents can be studied, as well as a range of cooling temperature-stress conditions that induce some fraction of radial hydride precipitation. Also, the response of the prehydrided and radial-hydride-treated (RHT) non-irradiated samples can be tested using high-displacement-rate ring-compression loading (≥ 0.01 m/s) and impact loading (2-3 m/s). Prehydriding, preconditioning and testing can be conducted rather quickly and inexpensively as compared to the radial-hydride treatment and testing of high-burnup cladding alloys. Currently, two of the three methods for radial-hydride treatment described in 3.3.2 and the impact testing described in 3.3.4 are available only for non-irradiated cladding alloys. Table 4 describes the hydrogen-content target ranges for cladding alloys. Because of sample-to-sample and alloy-to-alloy variation in surface conditions, the optimum conditions for prehydriding – hydrogen partial pressure, hold temperature, hold time, number of thermal and partial pressure cycles, etc. – are highly dependent on surface finish conditions and local variation in these surface conditions.

Table 4 Target Ranges of Hydrogen Contents for Cladding Alloys; HBR = H. B. Robinson type older Zry-4 with rough outer surface and etched inner surface; and BP = modern belt-polished alloys with grit-polished (sand-blasted) inner surfaces

Cladding Alloy	Design	Hydrogen Content, wppm			
		100±50	250±100	500±150	>650
HBR Zry-4	15×15	---	Yes	Yes	Yes
BP Zry-4	15×15	---	---	Yes	---
BP ZIRLO	17×17	---	Yes	Yes	---
BP Zry-2	10×10	Yes	Yes	---	---
BP M5	17×17	Yes	---	---	---

3.3.2 Preconditioning – Radial Hydride Treatment (RHT)

Three methods have been used in this work to induce radial hydrides by cooling under an applied hoop stress: (A) ring expansion using three-piece tooling; (B) cooling an open tube under constant internal pressure; and (C) cooling a sealed rodlet under decreasing internal pressure. Based on this experience, the sealed rodlet has been chosen as the reference for RHT.

A. Cooling under ring expansion loading using three piece tooling

This method is relatively fast and inexpensive. It is described in detail by Daum et al. ("Radial-hydride Embrittlement of High-burnup Zircaloy-4 Fuel Cladding," JNST, 43, No. 9 [2006] 1-14). Three-piece tooling (see Fig. 11) is positioned inside prehydrided and high-burnup HBR Zry-4 cladding rings (8-mm-long).

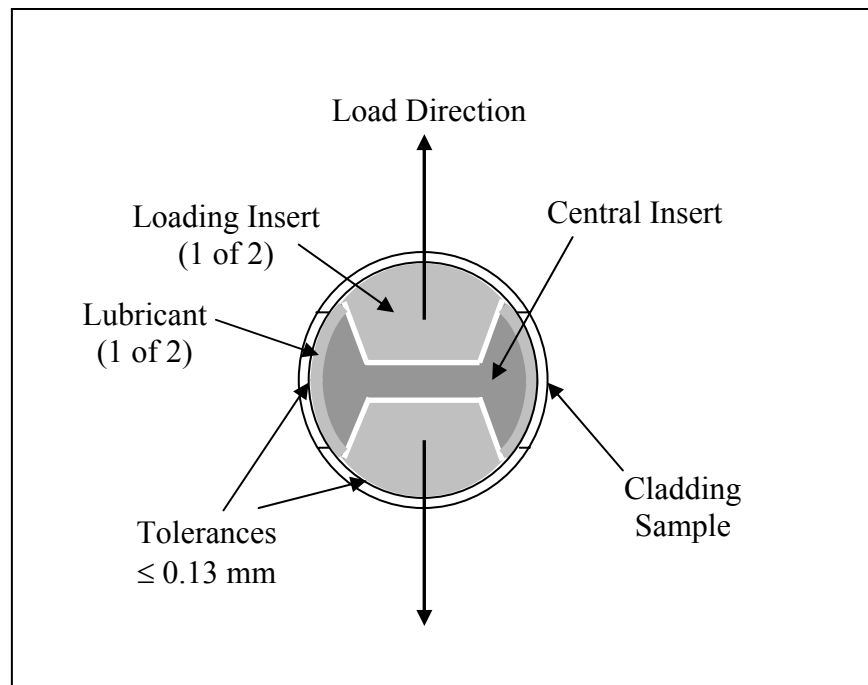


Fig. 11. Schematic of three-piece tooling used to induce hoop stress in cladding rings. The bottom insert is fixed. The central insert (dog-bone shape) can move upward. The load is applied to the top insert. For radial-hydride treatment, the Instron load-control mode is used to apply a force at 400°C, which remains constant during cooling.

As discussed by Daum et al., prehydrided samples have been heated to 400°C and held at 400°C for 1-2 hours. Just prior to initiation of cooling, the load corresponding to the desired mid-wall hoop stress is applied and held constant during cooling (15°C/minute to 200°C, slower rate from 200°C to RT). For high-burnup HBR cladding rings, the hold time was standardized to 2 hours at 400°C. Table 5 summarizes the hydrogen content and RHT for both prehydrided and high-burnup Zry-4. Also shown in Table 5 are the inner- and outer-surface hoop stresses in the cladding metal from ring-expansion tests at locations corresponding to the loading direction for

subsequent ring-compression tests. Because of bending, there is a stress gradient across the cladding wall that favors radial hydride formation during cooling near the inner surface and tends to suppress radial hydride formation near the outer surface. Although this artifact is undesirable, this RHT method has proven useful in determining the minimum local stress for radial hydride formation by means of hydride imaging and stress analysis. For constant load during cooling, the minimum local hoop stress for initiating radial hydride formation is 80 ± 10 MPa.

Table 5 Ring-stretch Hoop Stresses during Cooling from 400°C for Prehydrided HBR-type Zry-4 and High-burnup HBR Zry-4 Cladding Rings; samples were annealed at 400°C for 2 hours in the stress-free condition prior to cooling under constant wall-averaged hoop stress.

Cladding Type	H Content wppm	Mid-wall Hoop Stress MPa	Inner-Surface Hoop Stress MPa	Outer-surface Hoop Stress MPa
Prehydrided Zry-4	250-300	0	0	0
		40	115	<0
		60	125	<0
		90	160	30
		120	190	60
		150	215	95
Prehydrided Zry-4	>650	0	0	0
		90	160	30
		120	190	60
		150	215	95
High-burnup Zry-4 Corrosion Layer Intact	600-700	0	0	0
		90	160	30
		120	190	60
		150	215	95
High-burnup Zry-4 Corrosion Layer Removed	600-700	0	0	0
		90	160	30
		120	190	60
		150	215	95

B. Cooling under constant pressure using a one-side open tube

Creep samples HBR-C15 and S-C6 were cooled from 400°C and 380°C, respectively, under constant pressure. The average cooling rate to 200°C was $\approx 1^\circ\text{C}/\text{min.}$, while the cooling rate from 200°C to RT was $< 1^\circ\text{C}/\text{min.}$ This RHT method is better than the ring-stretch method because the pressure is controlled throughout cooling and the stress distribution across the thin-wall cladding is relatively uniform. Figure 3 shows the hydride morphology for HBR creep sample C15. The hydride morphology for the Surry creep sample is shown in Fig. 12. However, because the HBR C15 sample ruptured at 205°C during cooling, the creep apparatus, along with all of IML Cell #4, became highly contaminated. The constant-pressure creep furnaces and the laser-profilometer within the cell were dismantled and discarded as part of the decontamination process.

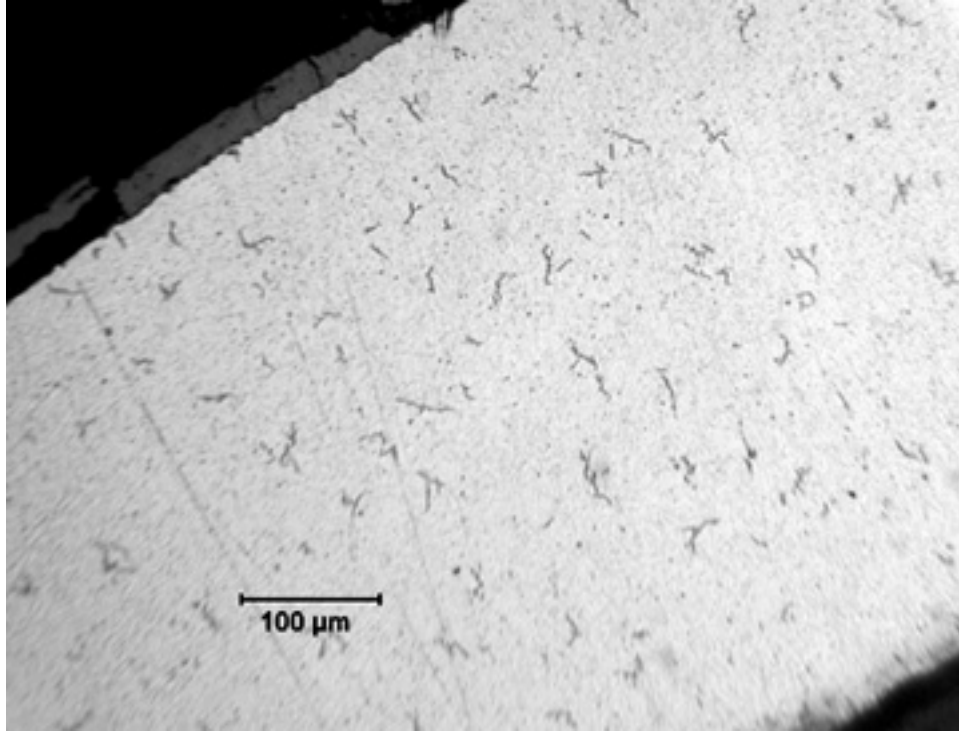


Fig. 12. Hydride precipitation in Surry Zry-4 cladding following creep testing at 380°C and 190 MPa for 2348 hours and cooling from 380°C to RT under constant pressure and at constant 190-MPa hoop stress; cooling rate to 200°C was $\approx 1^\circ\text{C}/\text{min}$. The hydrogen content within an adjacent sample was 130 wppm.

C. Cooling pressurized-and-sealed rodlets under decreasing pressure

RHT with a sealed rodlet has been selected as the reference method for the hydride reorientation study. The rodlet length is about 76-mm. One end is welded with an end-cap and two 25-mm-long zirconia pellets were inserted to minimize the stored energy inside the rodlet. The other end is then welded with a small breathe hole to allow pressurization at RT. RT pressures are chosen to give the desired hoop stress values (0-150 MPa) at 400°C. The rodlet with the small hole is inserted into a pressurization chamber, pressurized, and then laser-welded to seal the breathe hole. Three prehydrided Zry-4 rodlets were fabricated by this method with RT pressure levels designed to give cladding hoop stresses of 90, 120 and 150 MPa at 400°C. The rodlets were subjected to conditions intended to simulate drying operations: annealing for 3 days at 400°C and slow cooling to RT at 5°C/h. Because of the high creep rate of unirradiated, prehydrided Zry-4 and the small initial internal gas volume ($\approx 1.7 \text{ cm}^3$), RT hoop creep strains as high as 1.2% at the sample midplane were measured following cooling to room temperature. The increase in internal volume due to creep resulted in a decrease in cladding hoop stress (≈ 150 to ≈ 140 MPa) during the hold time and a faster decrease in stress during the slow 5°C/h cooling rate. As a result of this experience, one of the zirconia pellets ($\approx 1 \text{ cm}^3$ in volume) was removed to increase the RT internal volume to 2.7 cm^3 . With this modified design (see Fig. 13), outer diameter creep strains $< 2\%$ result in negligible increase in internal volume and decrease in hoop stress.

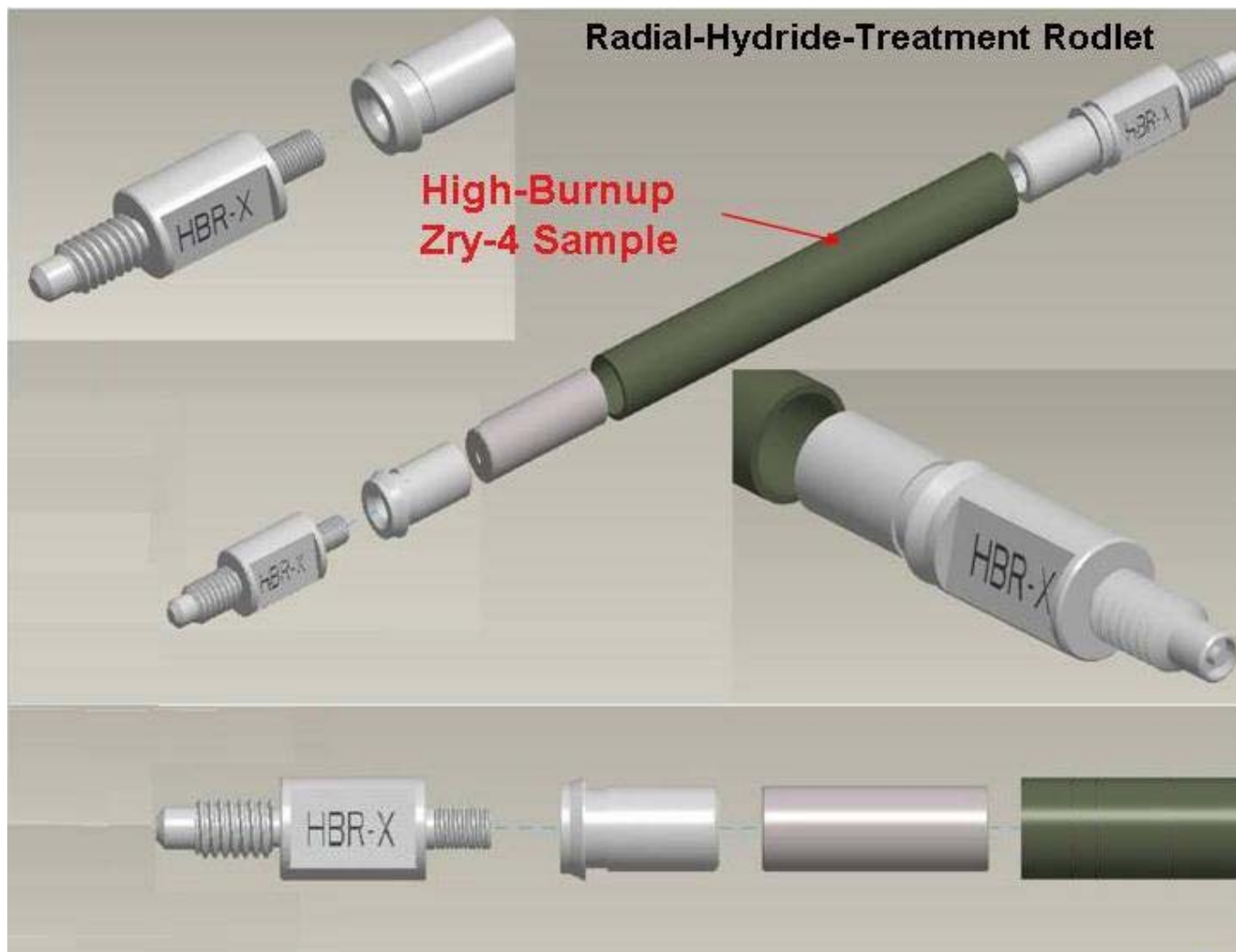


Fig. 13. New pressurized-and-sealed rodlet design for H. B. Robinson (HBR) Zry-4 cladding; new design uses only one 25-mm-long zirconia pellet inside the rodlet to increase internal volume and minimize relative volume expansion due to thermal creep.

Eleven rodlets with this new design feature were fabricated. Five of them have been exposed to different temperature histories (e.g., 0-3 h hold times at 400°C and 5-60°C/h cooling rates). Outer diameter creep strain profiles were measured for these new rodlets. Detailed finite element analyses were conducted to model each of these cases and to compare predicted creep strains to measured values, as well as to predict temperature and hoop-stress histories. Model-predicted creep rates were then adjusted to match the measured creep strains and the hoop stress history was recalculated. The results are summarized in Table 6. It is interesting to note that the creep strain of prehydrided ZIRLO is three times the creep strain for prehydrided Zry-4 under these short-time test conditions. Based on the analytical and experimental results, the optimum thermal history for nonirradiated, prehydrided cladding was determined to be: 1-h hold time at 400°C and 5°C/h cooling rate to 200°C, followed by stagnant-gas cooling to RT with the furnace power turned off.

Figure 14 shows that some radial hydrides precipitate during cooling from 400°C at 5°C/h with hoop stress decreasing from 150 MPa. However, the radial hydride fraction and continuity factor are relatively low compared to the results shown in Fig. 3 for cooling from 400°C at 1°C/min at higher *constant* stress (190 MPa). Ring-compression tests will likely show that the hydride morphology shown in Fig. 14 results in ductile behavior. The hydride-morphology results suggest that one-thermal-cycle drying operations at $\leq 400^\circ\text{C}$ and ≤ 150 MPa may not be sufficient to embrittle cladding. ISG-11, Rev. 3, does allow thermal cycling, which will be needed to dry high-burnup fuel assemblies, but it also limits the number of cycles (<10) for temperature drops per cycle $>65^\circ\text{C}$. Depending on the temperature variation per cycle, the radial hydride density may increase with each cycle. Thus, it is important to conduct RHT with thermal cycles. Consistent with ISG-11, Rev. 3, companion RHT tests will be conducted using 9 thermal cycles with a temperature drop of 100°C/cycle (i.e., 400°C to 300°C to 400°C) with a 6-minute hold at 400°C between cycles. The temperature-cycling RHT cases are indicated in Table 6 for prehydrided 15×15 BP Zry-4 and 17×17 ZIRLO cladding segments.

The ring-compression and crush-impact test results for the RHT rodlets shown in Table 6 will be used to determine the test conditions for high-burnup Zry-4 and ZIRLO rodlets. If thermal cycling does not produce significant radial hydride formation and significant decrease in ductility and failure energy, then only one-thermal-cycle 400°C and 150-MPa RHT will be conducted with high-burnup samples either for confirmation that high-burnup and prehydrided samples exhibit the same behavior or to determine differences in behavior between high-burnup and prehydrided cladding. If significant differences are observed, then tests with thermal cycling and <150 -MPa hoop stress will be conducted with high-burnup cladding samples.

Table 6 Test Matrix for Radial Hydride Treatment of Prehydrided Cladding Alloys using Pressurized-and-Sealed Rodlets; HBR = as-fabricated H. B. Robinson type cladding

Cladding	Hydrogen Content wppm	Hold Time at 400°C hours	Hoop Stress at 400°C MPa	Cooling Rate °C/h	OD Hoop Creep Strain %	Comment
15×15 Zry-4 (HBR-type)	170-350	0	150	4	0.5	---
15×15 Zry-4 (HBR-type)	1750 ^a	0	150	60	≤0.1	---
15×15 Zry-4 (HBR-type)	750±80	3	150	20	0.4	---
15×15 Zry-4 (HBR-type)	227-1460	1	150	5	0.4	Low radial hydride fraction for 410±50 wppm H
15×15 BP Zry-4	400 ^a	1	151	5	TBD	Radial Hydride Formation (TBD)
15×15 BP Zry-4	400 ^a	0.1 9 cycles 100°C/cycle	150	5	TBD	Radial Hydride Formation (TBD)
15×15 BP Zry-4	300 ^a	1	120	5	TBD	Radial Hydride Formation (TBD)
15×15 BP Zry-4	380 ^a	TBD	TBD	5	TBD	---
15×15 BP Zry-4	440 ^a	TBD	TBD	5	TBD	---
17×17 ZIRLO	400 ^a	1	150	5	1.4	Local H and radial hydride fraction (TBD)
17×17 ZIRLO	315 ^a	0.1 9 cycles 100°C/cycle	150	5	TBD	Radial Hydride Formation (TBD)

^aBased on sample weight gain.

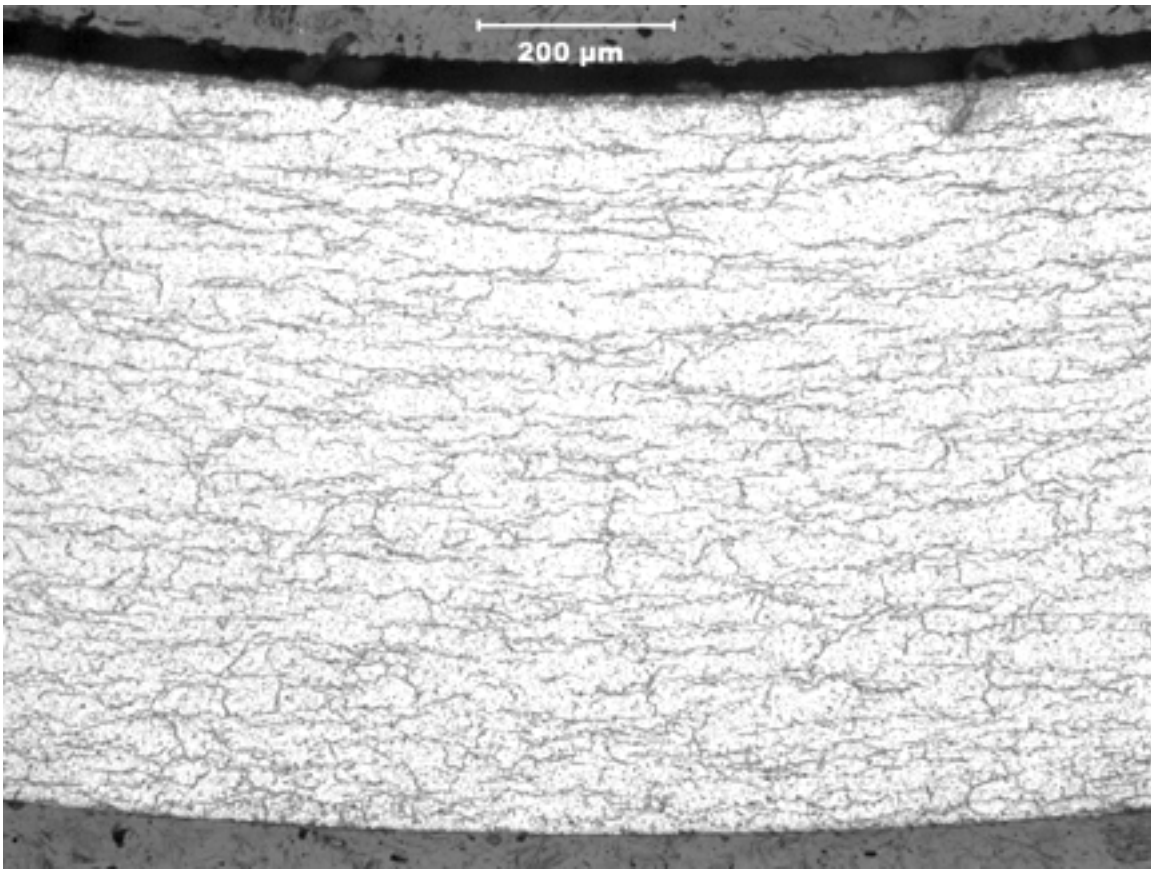


Fig. 14. Radial hydride formation in prehydrided (410 ± 50 wppm) HBR-type 15x15 Zry-4 subjected to the following RHT: 70-minute rise to 400°C, 1-hour hold at 400°C, 150 MPa average hoop stress after 1-h hold, cooling at 5°C/h to 200°C, and faster cooling from 200°C to RT.

3.3.3 Ring-compression screening tests

From the baseline and preconditioned samples, 8-mm-long rings are sectioned for ring compression testing, 2-mm rings are cut for hydrogen analysis and 4-mm rings are sectioned for metallography. Ring-compression ductility screening tests are performed at 150°C and a cross-head displacement rate of 10 mm/s ($\approx 100\%/s$ nominal strain rate in the loading direction). The Instron 8511 machine (see Fig. 9 for Instron and Fig. 15 for ring-compression loading) is used to test both nonirradiated and high-burnup cladding rings subjected to ring compression.

At such a high displacement rate, a displacement limit must be imposed prior to conducting the test to protect against the upper loading platen striking the lower support platen. A limiting displacement of 2 mm would be reasonable to allow for sufficient permanent displacement prior to failure. For HBR-type Zry-4, which has been tested at RT and 0.3%/s relative displacement rate, the permanent displacement following a total displacement of 2 mm was 1.2 mm (see Fig. 16), giving a relative permanent strain of $\approx 11\%$. The offset displacement, which traditionally represents the plastic displacement, is determined from the load-displacement curve and

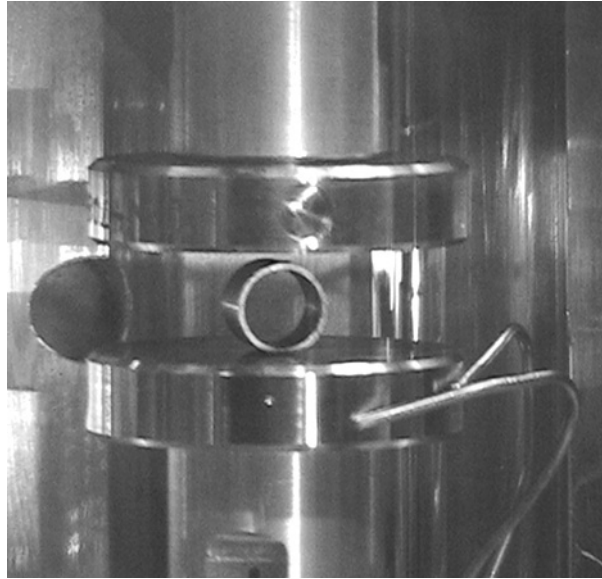


Fig. 15. View of Instron 8511 showing upper loading platen, ring sample and lower support platen with attached thermocouples.

confirmed by post-test diameter measurement, which gives permanent displacement. The offset and permanent displacements to the first through-wall crack (extending along the full 8-mm length) are normalized to the sample outer diameter to give nominal failure strain values. These failure offset and permanent strains are then compared to those measured for as-irradiated high-burnup Zry-4 rings and for the same material preconditioned at 0 MPa and 400°C. An appropriate metric (e.g., radial hydride density, radial hydride continuity factor, etc.) is determined from the metallographic images to correlate with ductility decrease. Ring-compression tests are repeated at 250°C for RHT that leads to a significant ductility decrease at 150°C. The approach is benchmarked using prehydrided, nonirradiated 15×15 Zry-4 cooled from 400°C at average hoop stresses of 90, 120 and 150 MPa. It is important to demonstrate that the ductility determined from ring-compression tests correlates strongly with preconditioning stress and with the hydride orientation and morphology determined from metallography. Such a benchmarking has been performed for prehydrided samples heated for 1-2 hours and cooled under constant average stress (60, 90, 120, and 150 MPa) induced by three-piece-tooling ring-stretch loading. However, such loading induces much higher bending stresses than would be encountered with pressurized-tube loading. It was difficult to induce radial hydrides across the wall of the cladding due to compressive bending stresses increasing from about the mid-radius to the outer surface. In most cases, the crack grew rapidly in the radial direction to about the mid-radius and then grew more slowly in the circumferential direction as the crack path branched from along radial hydrides to circumferential hydrides. Thus, the tests should be repeated using the pressurized-tube approach to generate a more uniform precipitation of radial hydrides across the cladding wall and a clearer correlation between ductility and hydride morphology.

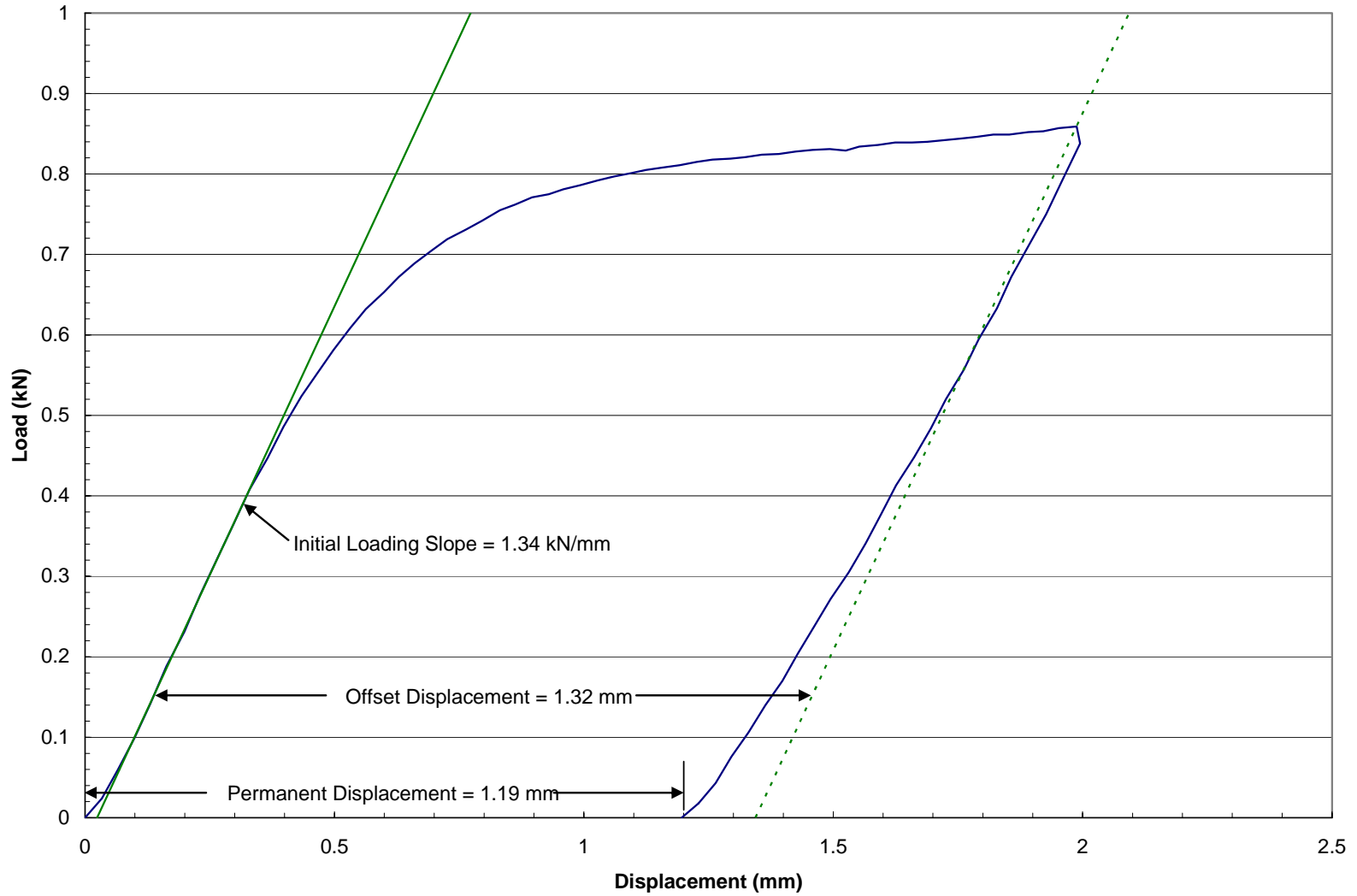


Fig. 16. Load-displacement results from RT compression and unloading of an 8-mm-long ring of HBR-type 15×15 Zry-4 cladding.

For samples that crack but do not fail through the wall following a total displacement of 2 mm, they are then subjected to ring-stretch tests to determine the average wall hoop stress at which through wall failure would occur due to gas pressure loading. This derived failure pressure is then compared to gas pressures anticipated in high-burnup rods following cooling to 150-250°C.

Based on testing already completed for prehydrided cladding and as-irradiated cladding, it is clear that the offset and permanent strains represent a combination of plastic deformation and crack displacement for samples that exhibit high deformation prior to failure. Such samples either have only circumferential hydrides or they have a brick-like structure of circumferential and radial hydrides. The circumferential hydrides tend to redirect crack growth from the radial direction to the circumferential direction. As such, it takes a higher energy input to fail these samples, as compared to highly brittle samples with only radial hydrides. For the SNF application, it is not important to separate out the energy that goes into plastically deforming the metal from the energy to partially crack the cladding. The offset strain and permanent strain to failure remain meaningful metrics to assess the performance of the preconditioned cladding. Perhaps a more meaningful metric is the area under the load-displacement curve up to the point at which the crack has penetrated through the wall thickness along the whole length of the sample. This failure energy (in J) can be normalized to the sample length (J/mm) and compared to failure energy under impact loading.

3.3.4 Impact Tests

The same basic approach used in 3.3.3 is used for impact failure-energy screening tests. Because of the geometry of the cladding, “standard” (e.g., Charpy) impact tests cannot be performed. For screening tests, it is sufficient to use the “product-impact-test” approach. As radial hydrides have the most degrading effect in response to hoop stresses, crush tests on 8-mm-long rings will be performed with a flat support plate and an impactor (tup) with a plate-like surface ($\approx 15 \times 15$ mm). Figure 17 shows a schematic of the apparatus prior to the impact test. Figure 18 shows the striker (tup) impacting the sample. (Note: both figures show a grooved support plate; this design has been changed to a flat support plate). The apparatus is designed to limit the impact displacement. To allow for direct comparison with ring compression tests, the displacement is limited to 2 mm. The testing method and analysis of results are benchmarked with as-fabricated, prehydrided (≈ 600 wppm), and prehydrided-RHT cladding samples impacted at room temperature. The recorded impact failure energy is used as the metric for cladding performance.

The impact test results at 2 m/s will be compared, in terms of failure energy, to the Instron ring-compression test results at 10 mm/s. If the sensitivity of failure energy to strain rate is small in this range, then it is possible that the impact tests are not needed. The ring-compression tests are performed in a servo-hydraulic Instron, encased in a glove box, capable of very high displacement rates ($\gg 10$ mm/s). The system has been designed for radioactive cladding and is operational. The cost for the radiologically controlled glove box was very high. It would be cost-prohibitive to design such a system for the impact tests. Also, the cost of a new impact

tester is relatively high (\approx \$100K). Before such investments are considered, it is important to determine whether or not impact testing is needed.

An existing impact tester, previously used for Charpy impact tests, has been refurbished and recalibrated to perform the initial set of tests with as-fabricated, prehydrided, and prehydrided-preconditioned Zry-4 (see Fig. 19 for close up view). For a pre-set height (h in Fig. 17), the velocity at which the tup impacts the sample is determined. The weight of the movable crosshead is chosen to give an impacting kinetic energy much greater than the impact energy needed to deform and fail the sample. As such, the tup moves at essentially constant velocity through the sample. The load-cell above the striking tup records load vs. time, which is then converted into load vs. displacement. By carefully choosing the area under part of this curve, the failure energy is determined. This failure energy is then compared to the results of the high-strain-rate ring compression test. If there is no significant difference in failure energy, then impact tests on irradiated cladding are not needed. For samples that do not fail within the 2-mm of tup-contact displacement, the maximum energy is simply determined by the area under the load-displacement curve and the failure energy is $>$ this maximum energy.

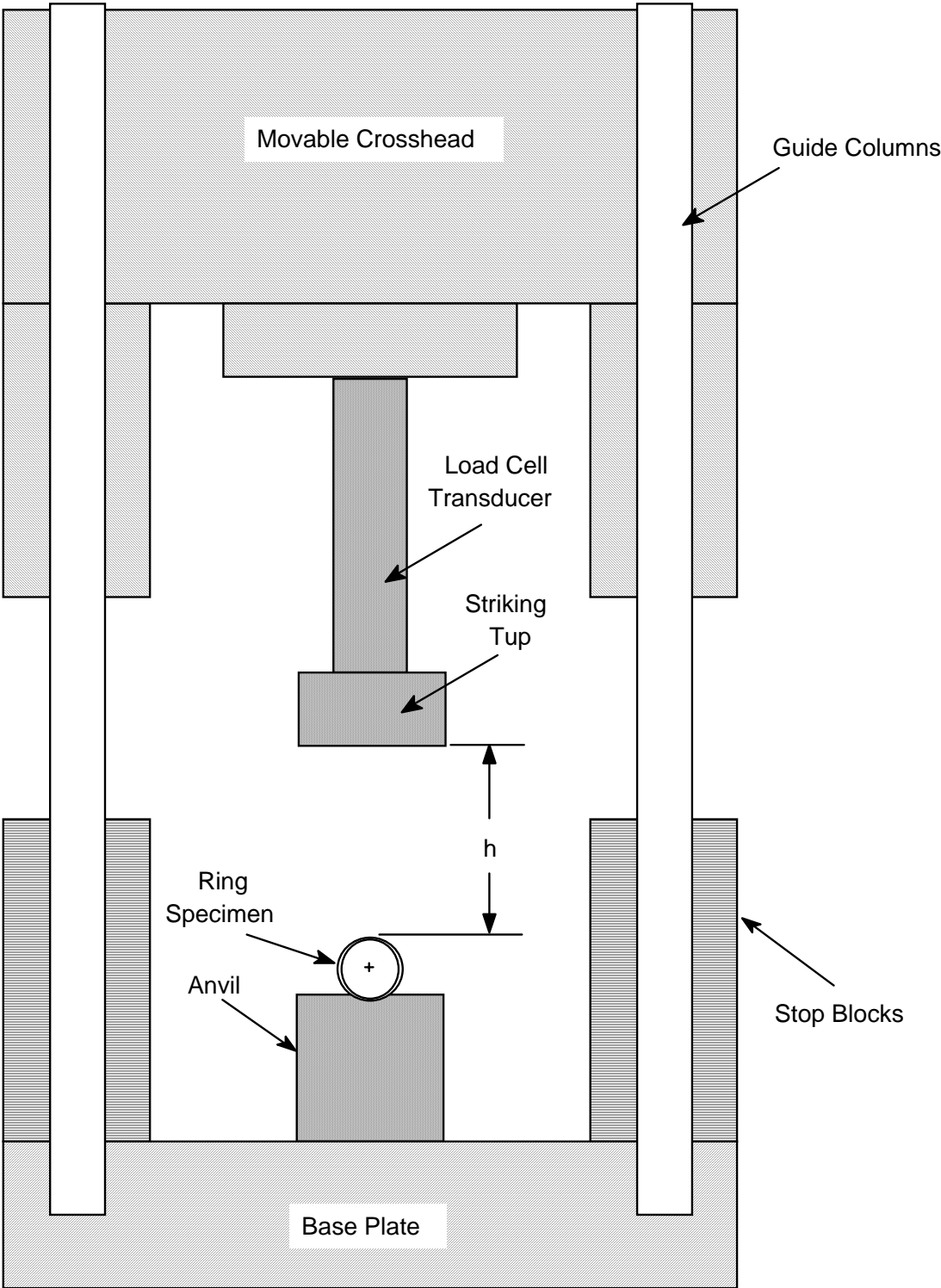


Fig. 17. Schematic of impact apparatus and sample prior to initiation of the crush-impact test.

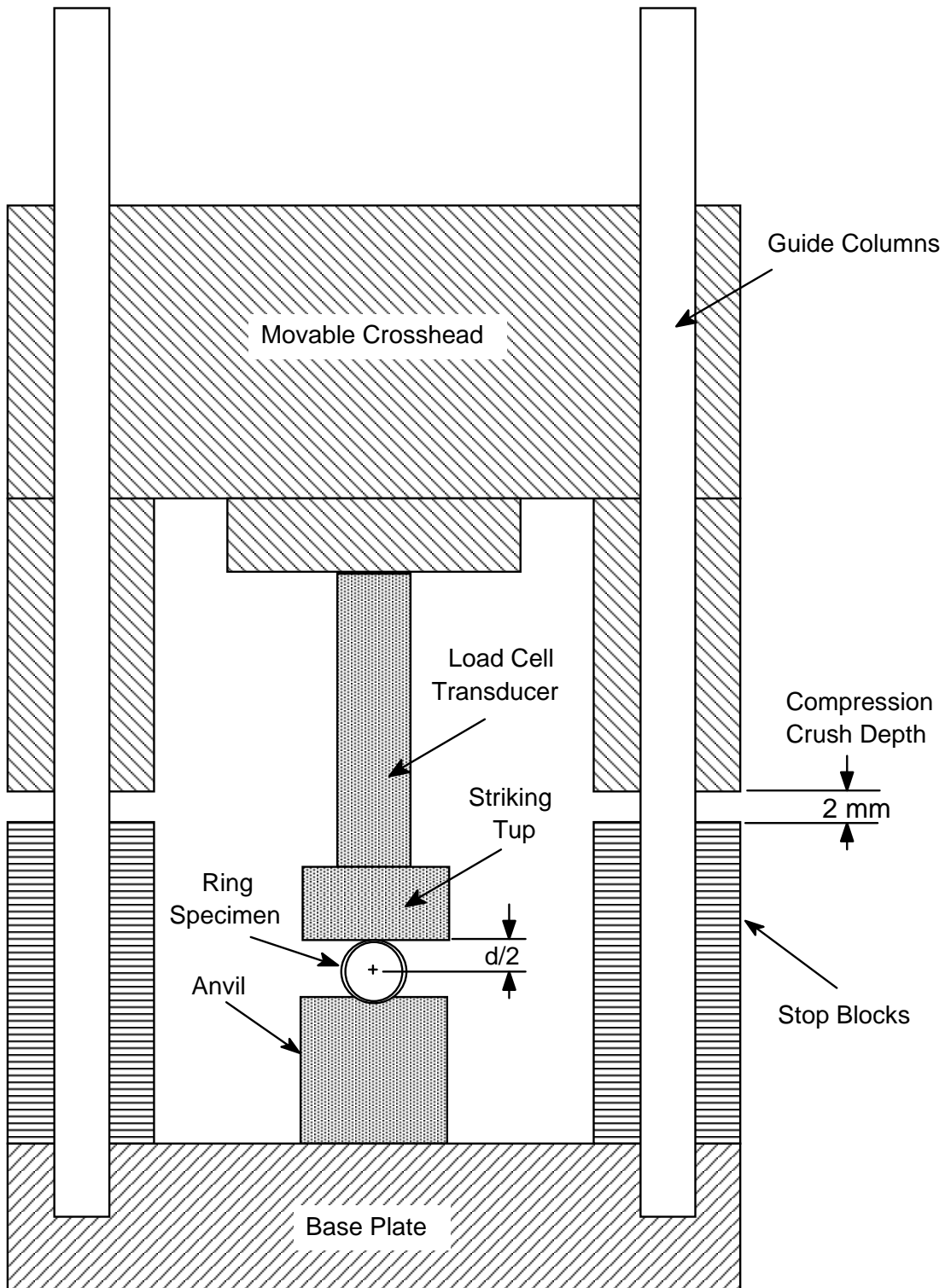


Fig. 18. Schematic of impact apparatus and sample at the moment of contact with the sample.



Fig. 19. Photograph of the refurbished impact test machine with the striking tup positioned on top of the ring for illustration purposes.

4. In-Cell Bending and Impact Tests with Fueled Cladding

Tests with longer (150-300 mm) segments of fueled cladding are very important to provide data needed to model the response of fuel rods to cask-drop events (normal \rightarrow HAC). However, these tests must be conducted in an alpha-gamma hot-cell workstation and relatively few of them

can be conducted. One of the tasks in the ANL-ORNL contract is for ORNL to determine testing scope, cost and schedule. At a minimum, RT bending and impact tests will be conducted with as-irradiated cladding samples. Preconditioning of fueled cladding samples to generate radial hydrides will be explored with ORNL. If the ANL results determine that significant radial-hydride formation is likely during slow cooling from 400°C at 150 MPa hoop stress (decreases as temperature decreases), then ANL and ORNL will determine a cost-effective way to RHT fueled-cladding segments.